

SPE/DOE 20241

Experimental Validation of a New Method for Optimizing Miscible Flooding of Stratified Reservoirs

P. Ingsøy, Rogaland Research Inst., and S.M. Skjæveland, Rogaland U. Centre

SPE Members

Copyright 1990, Society of Petroleum Engineers Inc.

This paper was prepared for presentation at the SPE/DOE Seventh Symposium on Enhanced Oil Recovery held in Tulsa, Oklahoma, April 22-25, 1990.

This paper was selected for presentation by an SPE Program Committee following review of information contained in an abstract submitted by the author(s). Contents of the paper, as presented, have not been reviewed by the Society of Petroleum Engineers and are subject to correction by the author(s). The material, as presented, does not necessarily reflect any position of the Society of Petroleum Engineers, its officers, or members. Papers presented at SPE meetings are subject to publication review by Editorial Committees of the Society of Petroleum Engineers. Permission to copy is restricted to an abstract of not more than 300 words. Illustrations may not be copied. The abstract should contain conspicuous acknowledgment of where and by whom the paper is presented. Write Publications Manager, SPE, P.O. Box 833836, Richardson, TX 75083-3836. Telex, 730989 SPEDAL.

1. ABSTRACT

Miscible displacement experiments were conducted in a stratified model reservoirs that permitted visual observation of the flow processes. Concentrating on favorable mobility ratio displacements, the results are analyzed by a VE theory which includes gravity effects^{1,2}. The results show that the front shape, and hence the recovery, of gravity stable displacements can be predicted by the theory. Further, rates for breakdown of gravity stabilization are predicted in agreement with experimental results. It is shown that channeling of the injection fluid into high permeability layers may be stabilized by viscous cross-flow, even during relatively high injection rates. Observation of unexpectedly large mixing zones are explained as viscous mixing caused by cross flow between layers.

2. INTRODUCTION

The vertical sweep efficiency obtained during miscible injection in stratified reservoirs with communicating layers depends on both gravity and viscous forces. The combined effect of these forces has been studied by numerical methods and in glass bead or sand models³⁻¹⁰. In some cases a *gravity stabilized* front may be obtained⁹. In other cases, gravity causes growing "fingers" (gravity over- or underdrive), or viscous forces cause the injection fluid to channel through high permeability layers. Some of these observations⁹, together with theoretical developments^{1,2,11}, suggest that important properties of the displacement may be quantitatively analyzed by methods based on the so-called vertical equilibrium (VE) assumption^{11,12}.

Treating immiscible piston-like displacements, Ekrann^{1,2} has used VE theory to describe the front shape, and hence recovery, in the *gravity stabilized* case. Further, he has predicted a critical injection rate above which gravity stabilization is not possible, and the injection fluid starts channeling into high permeability layers.

Experimental results are presented here to verify such applications of VE theory in miscible systems with gravity. The results are used also to discuss the development of a displacement under conditions when the theory does not apply. The focus in this study is on viscous and gravity forces only, mixing is neglected except for a

particular phenomenon associated with viscous mixing, discussed in Section 6.

Several experiments in stratified models have been reported in the petroleum literature. Starting in the fifties, experimenters have demonstrated the importance of cross-flow³ and gravity segregation^{4,5,6}. The presence of high permeability layers and the location of such layers have been shown to influence recovery severely in some cases⁵. Until recently, the experimental results were used qualitatively, or a physical model was used as an analog computer, and measured results were transformed by scaling rules and applied to the specific reservoirs.

Recently, attempts have been made to approach flooding of stratified models quantitatively with analytical methods⁷⁻¹⁰. Quintard et al.¹⁰ used the theory of large scale averaging to develop pseudo-properties, and was able to predict experimental water flood performance. Their solution, however, assumes that gravity can be neglected as compared with capillary forces. A successful quantitative treatment of the miscible case, including gravity, has, to our knowledge, not been presented.

Following Marle¹³ and Ekrann^{1,2}, we will adopt the following terminology: A displacement is said to be *stationary* if the front moves through the reservoir without changing its shape¹³. If the front is monotonically decreasing (slope always negativ) or monotonically increasing (slope always positiv), it is called *segregated*. A segregated stationary front is called *gravity-stabilized* if gravity causes the denser fluid to underdrive the less dense.

3. EXPERIMENTAL EQUIPMENT AND PROCEDURES

The experiments were carried out in a two-dimensional transparent cell using glass beads as the porous medium. Stratification was obtained by using different grade beads in the different layers. The cell was mounted vertically to allow for gravity effects. Fig. 1 shows the experimental system, and defines the coordinate system used in this study. The inner dimensions of the cell were 125 by 30 by 1.7 cm.

A packing technique¹⁴ was developed that produced bead packs

with porosities in the 36 - 38% range, and allowed the layers to be made with a fairly constant height (thickness), approximately ± 0.5 cm.

The displacement experiments were carried out using a salt solution and distilled water. Either the displacing or the displaced fluid were colored, and the displacement process was recorded by photographing or videorecording. Reasonable sharp fronts were usually observed so that the front position could be determined within a 3 - 5 cm interval. The pressure distribution in the cell could be measured through six holes (Shown in Fig. 1) drilled in the plastic plates and connected to differential pressure transducers or manometers. The pressure differences were relatively small, in the range 5 - 15 millibar, and considerable effort was needed to obtain reliable values.

The salt solution was made by dissolving sodium sulphate (Na_2SO_4) in water. The density was in the range 1.17-1.19 g/cm^3 . The viscosity was in the range 1.8 - 2.0 mPas, the 5% variation being introduced by room temperature and concentration variations. It follows that the mobility ratio can be estimated as

$$0.50 \pm 0.04,$$

in the favorable case, and

$$2.0 \pm 0.1,$$

in the unfavorable.

The model geometries under study were divided into four groups (G1-G4), see Table 1. Note that the layers are numbered from the bottom an up. The porosities of the different layers could not be measured accurately in the cell, and were therefore determined from separate porosity measurements in columns. The results are given in Table 1. The error introduced by using the column results can be assumed to be small, i.e. some 5%, since the porosity of normally packed glass beads do not vary a great deal¹⁵.

The permeabilities of the bead packs (Table 1) were measured in-situ using a dye as a nonadsorbing tracer in the distilled water to obtained the average fluid velocity directly. These displacements were also used as quality control of the uniformity of each layer in the bead pack. The permeability measurements are expected to be accurate within 10%.

Most of the experiments were duplicated, and the results from the second displacement were always consistent with what had been previously obtained.

4. VERTICAL EQUILIBRIUM THEORY

A Vertical Equilibrium theory may be developed based on the assumption that sum of all fluid driving forces in the vertical (cross-dip) direction is zero¹². A consequence of this is that the flow-potential must be a function of x only^{1,2,12}:

$$\varphi_j = \rho_j (p_j + g_x x + g_y y) \quad (1)$$

Here ρ_j is the density of phase j and p_j is the pressure. g_x and g_y are the x and y components of gravity.

Defining the reservoir effective length to height ratio as

$$R_L = \frac{L}{H} \left(\frac{k_y}{k_x} \right)^{1/2} \quad (2)$$

where L is the length (along stratification) of the reservoir, H is the height, and the average permeabilities are defined as

$$\bar{k}_x = \frac{1}{H} \int_0^H k_x dy \quad (3)$$

$$\bar{k}_y = \frac{H}{\int_0^H \frac{1}{k_y} dy} \quad (4)$$

Zapata and Lake¹¹ have shown that the VE assumption is a reasonable approximation for viscously-dominated cases provided R_L is greater than about 10. Note from Table 1 that models used in this study had R_L ratios significantly lower than this, i.e. in the range 2.5 - 3.6.

Assuming the distribution of saturation in the reservoir is given (a degree of freedom that must be removed later for practical applications), it is a simple task to develop an expression for u_{jx} , the x component of the fluid darcy velocity anywhere in the reservoir¹². This result can be used to develop a method based on pseudo-functions. We choose not to follow this path in the analysis of our data, since it can be shown¹³ that the introduction of significant gravity effects may make the equation for the pseudo-saturation parabolic and hence unsuited for the method of characteristics.

Analyzing immiscible displacements, Ekrann's theory is restricted to *monotonically decreasing or increasing* fronts which locally are considered to be piston-like^{1,2}. The fluid are considered incompressible. Mathematically, he arrives at VE by taking the limit of infinite permeability in the vertical (y) direction. In the absence of dispersion, Ekrann's results may be applied directly to the miscible case.

Under the assumption of infinite vertical permeability, Ekrann develops an equation describing the shape of a gravity-stabilized decreasing front^{1,2}. With the definitions given in Appendix 1, this equation can be written:

$$\frac{\partial h^{(0)}}{\partial x} = \frac{q}{\Delta z \Delta \rho g_y \pi_T} \left(\frac{\pi_u}{a_u} - \frac{\pi_o}{b_o} \right) - \frac{g_x}{g_y} \quad (5)$$

Here, $h(x,t)$ is a function describing the front (Fig. 1), q is the volumetric injection rate and Δz is the extension of the reservoir in the z -direction. $\Delta \rho$ is the density difference defined as the density of the displacing fluid minus the density of the displaced fluid. The functions denoted π (with subscript) represent integrals over the reservoir porosity, and the functions denoted by a and b (with subscripts) represent integrals over the mobility of the displacing and displaced fluid, respectively. Note from Appendix 1 that the only free variable at the right hand side of Eq. 5 is x which appears through $h^{(0)}(x)$. We will refer to the solution given by Eq. 5 as the $VE^{(0)}$ solution.

Eq. 5 gives the solution for a monotonically decreasing front. The corresponding equation for an increasing front is obtained by interchanging subscripts u and o .

Eq. 5 holds strictly for the case of infinite permeability in the y -direction. Ekrann^{1,2} uses this solution to develop an approximation, $h^{(1)}(x,t)$, for the real front, $h(x,t)$, in a system with finite vertical permeability:

$$\frac{\partial h}{\partial x} \sim \frac{\partial h^{(1)}}{\partial x} = \frac{-\Delta\rho g_y}{\frac{u_{ya}^{(0)}}{\lambda_{ya}} - \frac{u_{yb}^{(0)}}{\lambda_{yb}} - \Delta\rho g_y} \frac{\partial h^{(0)}}{\partial x} \quad (6)$$

Here, and in the following, subscripts *a* and *b* denote displacing and displaced fluid, respectively. $u_{ya}^{(0)}$ and $u_{yb}^{(0)}$ are the *y* components of the darcy velocity at the point $(x, h(x))$ on the front, calculated for the infinite vertical permeability case (Eq. 5), see Appendix 1. λ_{ya} and λ_{yb} are the mobilities at the same point. In the following, the solution given by Eq 6 is referred to as the VE⁽¹⁾ solution.

Eq. 6 is based on requiring pressure continuity along the displacement front $h^{(1)}(x, t)$ in the system with finite vertical permeability, while approximating the darcy velocities at the front with the VE⁽⁰⁾ velocities.

We extend the theoretical model slightly by repeating this argument, again requiring pressure continuity, and using the velocities $u_{ya}^{(1)}$ and $u_{yb}^{(1)}$ calculated from the VE⁽¹⁾ solution (See Appendix 1), to develop a new approximation of the front:

$$\frac{\partial h}{\partial x} \sim \frac{\partial h^{(2)}}{\partial x} = \frac{-\Delta\rho g_y}{\frac{u_{ya}^{(1)}}{\lambda_{ya}} - \frac{u_{yb}^{(1)}}{\lambda_{yb}} - \Delta\rho g_y} \frac{\partial h^{(1)}}{\partial x} \quad (7)$$

We will refer to the solution given by Eq. 7 as the VE⁽²⁾ solution.

Eqs (5) - (7) have been developed for monotonically decreasing or monotonically increasing fronts. Ekraan points out that for a given reservoir geometry, the front slope given by Eq. 6 may change sign if the injection rate exceeds a certain critical rate. At this rate the theoretical description breaks down, and Ekraan assumes that at this rate gravity stabilization breaks down, and the injection fluid starts channeling into a high permeability layer, i.e forming a non-gravity tongue^{1,2}.

By inspecting the signs of the left sides of Eqs. 6 and 7, we are now in position to determine two critical rates, termed $q_c^{(1)}$ and $q_c^{(2)}$, for breakdown of gravity segregation. These will be compared with experimental results in the following section.

5. EXPERIMENTAL RESULTS

Most of the results given here are from displacements with favorable mobility ratio. Data are first presented to justify the use of Eqs. 5 and 6 to describe gravity stabilized displacements. Next, we consider the breakdown of gravity stabilization, and compare with predictions produced by Eqs. 6 and 7. Finally, we discuss the development of displacements at large rates which prevented gravity stabilization.

An overview of the experiments is given in Table 2. The injection rates were in the range 0.17 - 1.0 cm³/min. The injection rates should be multiplied by 2.6 to obtain the (approximate) average front velocity in ft/day.

Injection rates in the 0.17 to 0.2 cm³/min range are referred to as *low rates*, rates in the 0.42 - 0.5 cm³/min range are called *medium rates*, and rates higher than 0.8 cm³/min are denoted *high rates*.

5.1 Favorable mobility ratio

5.1.1 Gravity dominated displacement

In these displacements, with *M* close to 0.5, the dense fluid displaced the less dense, and gravity stabilization required gravity override.

Stationary fronts were observed in all the low rate displacements except Experiment 3 where the predicted gravity stabilized front was longer than the model reservoir. The observed stationary front shapes agreed reasonably well with predictions based on Eqs. 5 and 6, *except* for points near the boundaries between the layers. Here, thin tongues were observed to form, see Figs. 2 and 4. The tongues were some 1-3 cm thick, but did stabilize. In spite of these tongues (which strictly violate the requirement of gravity segregation) we still classify these fronts as gravity-stabilized.

As seen from Fig. 2, Experiment 1, the predictions based on Eqs. 5, 6 and 7 agree reasonably well with the observations, the differences between the three theoretical predictions being small. From Table 2, the rate, 0.167 cm³/min (0.44 ft/day), was well below the predicted rates for breakdown of gravity stabilization. Figure 2 confirms that in this case the recovery can be approximately calculated by integration of Eq. 5 or 6. The results obtained from Experiment 1 are consistent with preliminary results from a nearly similar experiment, presented in Ref 9.

Fig. 3, Experiment 2, shows a gravity stabilized front obtained in a three layer reservoir with the most permeable layer at the top. Some dispersion was present in the bottom layer, preventing determination of the front position, but it can be seen that the theoretical predictions are in good agreement with the observations of the front in the two upper layers. The reason for the dispersion is not understood, but gravity dominated displacements in three layer reservoirs repeatedly to produce some dispersion in the lower layer. (Compare Fig. 4).

Another low rate displacement, Experiment 3, was carried out in an approximately symmetric three layer model (Table 2), the middle layer being the most permeable. The predicted gravity stable front was significantly longer than the reservoir length. However, the data show that stabilization was obtained in the two lower layers of the reservoir, and the front can be labelled *partially stationary*. In the upper layer the front shape was observed to change in direction of the predicted stationary front. The stationary part had a shape that agrees well with the theoretical prediction, see Fig. 4. It should be noted that the injection rate again was well below the critical rates, see Table 2

5.1.2 Breakdown of gravity segregation

The VE theory predicts that gravity segregation will break down at a certain critical rate, and that a tongue will start growing^{1,2}. The experiments showed that in the favorable mobility ratio case, the breakdown of gravity segregation is a more gradual process. A small tongue formed usually at a rate lower than that predicted by Eq. 6 but more consistent with the rate predicted by Eq. 7.

This is illustrated by Experiments 4, Fig. 5, and Experiment 5, Fig 6. In Experiment 4, the critical rate is predicted by Eq 6 to 0.62 cm³/min and by Eq 7 to 0.35 cm³/min, see Table 2. The observations show that at a rate of 0.42 cm³/min, a tongue started to grow in the high permeability layer and introduced a positive front slope. The tongue stabilized and the front reached a stationary shape, even though a barely visible dispersed zone with very low salt concentration was formed in front of the tongue. The stabilization of the tongue is believed to be caused by the combined action of viscous cross flow and gravity, as will be discussed in Section 6. Note from Fig. 5 that the theoretical prediction based on

Eq. 5 or 6 is still in good agreement with the observations in spite of the tongue.

In the medium rate Experiment 5, Fig. 6, gravity segregation again broke down at a rate lower than predicted by Eq. 6 but consistent with Eq. 7. Also in this experiment the front reached a stationary shape.

In Experiment 6, which was performed in the same three layer model reservoir as Experiment 2, the front behaved qualitatively similar to what was observed in Experiment 4. A small tongue developed at medium rates in the middle layer, and some dispersion was observed in front of it. In spite of this the front again reached a stationary shape.

5.1.3 High rate displacements

High rate displacements were performed in Experiment 7, Fig. 7, and Experiment 8, Fig. 6. A spectacular feature of the high rate displacements with high permeable layers at the top, was the development of a mixing zone extending in front of the tongue, Fig. 7. This phenomenon is discussed in Section 6. The mixing zone appeared from visual observations to carry only a small fraction of the salt concentration of the injected fluid, and, as a matter of terminology, is not considered here as part of the front, see Fig. 7. In spite of the mixing zone it was generally possible to determine the position of the displacement front with reasonable accuracy (some 3 - 5 cm).

An example of this is shown in Fig. 7, Experiment 7. The tongue in the high permeability layer grew to a certain length before the growth ceased and the front maintained a stationary shape.

A less pronounced mixing zone was produced in front of the tongue that developed in the high rate displacement shown by Fig. 6, Experiment 8. Again the front was observed to reach a stationary shape.

5.2 Unfavorable mobility ratio

The unfavorable mobility ratio displacement reported here, Experiment 9, was performed in a model reservoir with the high permeable layer at the bottom, Fig. 8. Gravity stabilization in this case would require gravity override. However, gravity stabilization was not expected due to Eq. 5 which predicts infinitely long gravity stabilized fronts in this geometry. This was consistent with the experimental results in the sense that no stationary fronts were observed. The front shapes however, in the low rate displacements were seen to change in the direction of the predicted gravity stable front.

Fig. 8 shows an example of a high rate displacement. The front was observed to change in the direction of the predicted gravity stable front except for a tongue that started to grow as expected by Eq. 7, see Table 2. However, in the high rate displacements with mobility ratio close to 2, no mixing zones were produced by the growing tongues. Nor did the tongues stop growing, but continued extending in length until break-through. Note that the high rate in this case was below the $VE^{(0)}$ critical rate (from Eq. 5).

6. DISCUSSION

The VE theory of gravity stabilization, see Section 4, can not explain the stationary fronts with stable tongues obtained during the high rate displacement experiments. An explanation of these observations must likely take viscous cross flow into account. Disregarding gravity (and capillary forces) another type of VE model has been discussed by Zapata and Lake¹¹, who have shown that in the $M < 1$ case viscous cross-flow may suppress the effect of heterogeneities, and can in an idealized VE case, cause the displacement front to move with the same velocity in the high and low permeability layers^{11,12}.

Considering as an example Fig. 9, the arrows indicate the direction of the viscous cross-flow generated. It is clear from Fig. 9 that the cross-flow suppresses the front velocity difference in the two layers. However, it should be noted that the criterion given by Lake¹², for obtaining equal front velocities,

$$M < \frac{k_2 \phi_1}{k_1 \phi_2} \quad (8)$$

was not satisfied, neither in Experiment 7 nor 8. This may indicate that the combined effect of gravity and viscous cross-flow must be taken into account to explain the stabilization.

The cross flow also offers an explanation of the spectacular mixing zone which was observed in the high permeability layers in several high rate floodings (see Fig. 7 and Ref.9), and to a lesser degree in some medium rate displacements (Fig. 5). Considering the small dispersivity of glass beads, and the dispersion usually observed in the experiments presented here, the extension of the mixing zone shown by Fig. 7 is very much larger than expected.

A close inspection of the mixing zone reveals a fingering structure with fingers extending up and downstream in the (qualitatively) expected direction of the cross-flow, see Fig. 9. The width of the fingers was typically 2 - 3 cm in the high rate displacements exemplified by Experiment 7, Fig. 7.

Considering the geometry of the front, Fig. 9, the development of fingers seems understandable since the denser fluid was overlying the less dense, and since the cross-flow directed the water up into the more dense and viscous injected fluid. As to the effect of gravity, it should be noted that a similar mixing zone did not develop in the high rate Experiment 8, Fig. 8, and similar cases with $M > 1$, even if the gravity effect should be the same.

Development of mixing zones due to viscous cross-flow has been suggested earlier on the basis of numerical simulation and theoretical arguments¹¹, and may conveniently be termed *viscous mixing*. This is to our knowledge the first experimental account of what is probably such a phenomenon. From our experimental observations we suspect the mixing zone to improve the sweep efficiency by taking part in stabilizing the displacement, but this assumption should be confirmed by further research.

Starting an experiment, we carefully tried to establish a monotonically decreasing or increasing front which at a certain time was defined as the initial condition or *initial front* at $t=0$. However, due to the stratification of the media, this was not always possible, and small tongues would be present at the start of the experiment. This poses the question whether the initial front shape had an significant influence on the final outcome of the experiment.

In the favorable mobility ratio displacements this did not seem to be the case. Several experiments with slightly different initial conditions always produced essentially the same result with respect to gravity stabilization, growing or non-growing tongues etc.

For unfavorable displacement, however, preliminary results indicate that growing tongues developed in some displacements at lower rates than expected, depending on the steepness of the initial front. These observations, which will be presented in a subsequent publication, may for the $M > 1$ case, to limit the value of the VE theory presented in Section 4. The difference between favorable and unfavorable displacement in this respect, is believed to be related to the mechanisms preventing tongues to grow in the $M < 1$ case.

7. CONCLUSIONS

Presenting experimental results, we have shown that miscible displacements in stratified model reservoirs can be analyzed

successfully by VE theory in the case of significant gravity effects, and effective reservoir length to height ratios in the 2.5 - 3.6 range.

For the favorable mobility ratio case, we have shown that:

1) The front shape of gravity stabilized displacements could be predicted by the VE theory, and recovery can be estimated from Eq. 5.

2) Breakdown of gravity segregation, was successfully predicted by the theory, Eq. 7. For injection rates exceeding those predicted by Eq. 7, the injection fluid started to form a tongue extending into the high permeability layer (channeling).

3) Tongues formed after breakdown of gravity segregation were shown to be stabilized. Viscous cross flow is believed to contribute to the stabilization.

4) Cross-flow was observed to produce large viscous mixing zones in high permeable layers. The extension of these zones was very much larger than expected on the basis of ordinary (1D) dispersion models.

For the unfavorable mobility ratio case it was shown that breakdown of gravity segregation in high rate displacements resulted in growing tongues that did not stabilize. Disregarding the tongues, the rest of the displacement front was observed to change in the direction of the predicted gravity stable front.

8 NOMENCLATURE

Symbols

a	= Integral over mobility, displacing fluid
b	= Integral over mobility, displaced fluid
Δz	= Reservoir extension in the z-direction
g	= Gravity
H	= Reservoir height
h	= Function describing the displacement front
k	= Permeability
L	= Reservoir length
M	= Mobility ratio
p	= Pressure
q	= Volumetric injection rate
R_L	= Effective length to height ratio
t	= Time
u	= Darcy velocity
x	= Spatial coordinate
y	= Spatial coordinate
ϕ	= Porosity
φ	= Flow potential
λ	= Mobility
μ	= Fluid viscosity
π	= Integral over porosity
ρ	= Fluid density

Superscripts:

- (0) = Calculated from the VE⁽⁰⁾ solution.
 (1) = Calculated from the VE⁽¹⁾ solution.
 (2) = Calculated from the VE⁽²⁾ solution.

Subscripts:

a	= Displacing fluid
b	= Displaced fluid
c	= Critical
j	= Fluid phase

o	= Over front
T	= Total
u	= Under front
x	= x component
y	= y component

9. ACKNOWLEDGEMENT

The authors would like to thank Prof. Larry Lake of the University of Texas for his help and cooperation, and Paul Goonewardene of Rogaland Research Institute for assisting the laboratory work. We acknowledge the support of The Norwegian State Research and Development Program for Improved Oil Recovery and Reservoir Technology (SPOR), The Royal Norwegian Council for Scientific and Industrial Research, and The Norwegian Research Council for Science and the Humanities.

10. REFERENCES

- Ekran, S., "An Analysis of Gravity-Segregated Piston-Like Displacement in Stratified Reservoirs", SPE 18598, paper submitted to *SPE Reservoir Engineering*.
- Ekran, S., "Om flømming av stratifiserte reservoarer", report to SPOR, Rogaland Research Institute, Stavanger (1986).
- Van Meurs, P., "The Use of Transparent Three-Dimensional Models for Studying the Mechanism of Flow Processes in Oil Reservoirs", *Trans. AIME* (1957), 295-301.
- Gaucher, D. H. and Lindley, D. C., "Waterflood Performance in a Stratified, Five-Spot Reservoir - A Scaled-Model Study," *Trans. AIME* (1960), 219, 208-215.
- Richardson, J. G. and Perkins, F. M., "A laboratory investigation of the Effect of Rate on Recovery of Oil by Water Flooding," *Trans. AIME* (1957), 210, 114-121.
- Craigh, F. F., et al., "A Laboratory Study of Gravity Segregation in Frontal Drives," *Trans. AIME* (1957), 210, 275-281.
- Wright, R. J. and Dawe, R. A., "Fluid Displacement Efficiency in Layered Porous Media; Mobility Ratio Influence," *Rev. Inst. Fr. du Petrole* (1983), 38, 455-474.
- Amhed, G., et al., "An Experimental Study of Waterflooding From a Two-Dimensional Layered Sand Model," *SPE* (Feb. 1988), 45-54.
- Ingsøy, P. and Ekran, S., "Laboratory studies of miscible displacement in two-dimensional layered reservoirs," *Proc.*, 3th International Symposium on Enhanced Oil Recovery, February 19-22, 1989, Maracaibo.
- Quintard, M., et al., "Two-Phase Flow in Heterogeneous Porous Media; The Method of Large-Scale Averaging Applied to Laboratory Experiments in a Stratified System," SPE 19682 presented at the 64th Annual Technical Conference of the Society of Petroleum Engineers, San Antonio, October 8-11, 1989.
- Zapata, V. J. and Lake, W. L., "A theoretical Analysis of Viscous Crossflow", SPE 10111 presented at the 56th Annual Technical Conference of the Society of

Petroleum Engineers, San Antonio, October 5-7, 1981.

12. Lake, L., "Enhanced Oil Recovery", *Prentice Hall* (1989), New Jersey.
13. Marle, C. M., "Multiphase Flow in Porous Media," *Technip* (1981), Paris.
14. Ingsøy, P., "A 2D flooding rig for stratified porous media", report SPOR 3/88 (1988), Rogaland Research Institute, Stavanger.
15. Churchill, S. W., "Viscous Flows," *Butterworths Series in Chemical Engineering* (1988), Stoneham, MA.

APPENDIX 1

Assuming that the displacement front is described by the function $h(x,t)$ (Fig. 1), and denoting the *displacing* fluid with the letter a , and the *displaced* fluid by b , we introducing the following notation for mobility integrals:

$$a_o = \int_h^H \frac{k_x}{\mu_a} dy \quad (A1)$$

$$b_o = \int_h^H \frac{k_x}{\mu_b} dy \quad (A2)$$

$$a_u = \int_0^h \frac{k_x}{\mu_a} dy \quad (A3)$$

$$b_u = \int_0^h \frac{k_x}{\mu_b} dy \quad (A4)$$

Integrals over porosities are denoted:

$$\pi_o = \int_h^H \phi dy \quad (A5)$$

$$\pi_u = \int_H^h \phi dy \quad (A6)$$

$$\pi_T = \pi_u + \pi_c \quad (A7)$$

Assuming VE i.e. the flow potential is a function of x only, it is straight forward to calculate the x -components of the darcy velocities^{1,2,12}. Here, Ekkrann's results^{1,2} for decreasing fronts are given, the corresponding expressions for increasing fronts are obtained by interchanging subscripts o and u .

$$u_{xa} = \lambda_{xa} \frac{\frac{q}{\Delta z} + \Delta \rho b_o \left(g_x + \frac{\partial h}{\partial x} g_y \right)}{a_u + b_o} \quad (A8)$$

and

$$u_{xb} = \lambda_{xb} \frac{\frac{q}{\Delta z} - \Delta \rho a_u \left(g_x + \frac{\partial h}{\partial x} g_y \right)}{a_u + b_o} \quad (A9)$$

If the front is stationary and described by $h^{(0)}(x,t)$, $h^{(1)}(x,t)$ or $h^{(2)}(x,t)$, we mark the corresponding velocities by superscripts (0), (1) and (2). For points at a stationary front, the y components of the velocities can be found by^{1,2}:

$$u_{ya}^{(0)}(x,h) = \frac{\partial h^{(0)}}{\partial x} \left(u_{xa}^{(0)} - \phi \frac{q}{\Delta z \pi_T} \right) \quad (A10)$$

and

$$u_{yb}^{(0)}(x,h) = \frac{\partial h^{(0)}}{\partial x} \left(u_{xb}^{(0)} - \phi \frac{q}{\Delta z \pi_T} \right) \quad (A11)$$

TABLE 1

Reservoir model properties

Geo- metry	Layer No (Bottom = 1)	Porosity	Perm. (darcy)	Height (cm)	R _L
G1.1	1	0.36	1.8	21.0	3.5
	2	0.38	6.8	8.0	
G1.2	1	0.36	1.8	20.5	3.2
	2	0.38	8.7	8.5	
G2	1	0.36	1.8	11.0	2.5
	2	0.38	3.2	9.6	
	3	0.36	24.0	7.8	
G3	1	0.36	1.7	10.2	3.6
	2	0.36	5.5	10.2	
	3	0.38	1.9	8.5	
G4	1	0.38	1.8	10.5	3.4
	2	0.36	6.9	18.5	

TABLE 2

Summary of experiments

Expe- riment	Geo- metry	Rate (cc/min)	qc(1) (cc/min)	qc(2) (cc/min)	Observations
1	G1.1	0.17	0.62	0.35	Gravity stable
2	G2	0.20	0.64	0.39	Gravity stable. Dispersion in lower layer.
3	G3	0.20	0.71	0.43	Partially gravity stable
4	G1.1	0.42	0.62	0.35	Breakdown of gravity- segregation, stationary front.
5	G3	0.50	0.71	0.43	Breakdown of gravity- segregation, stationari front.
6	G2	0.50	0.64	0.39	Breakdown of gravity segregation, stationary front.
7	G1.2	1.00	0.58	0.35	Breakdown of gravity segregation, stationary front, large mixing zone.
8	G3	1.00	0.71	0.43	Breakdown of gravity segregation, stationary front, mixing zone.
9.	G4	1.00	1.27	0.85	Breakdown of gravity segregation, growing tongue.

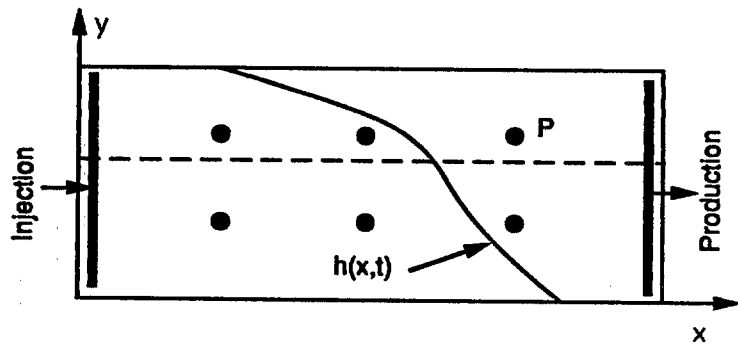


Fig. 1 - Experimental system

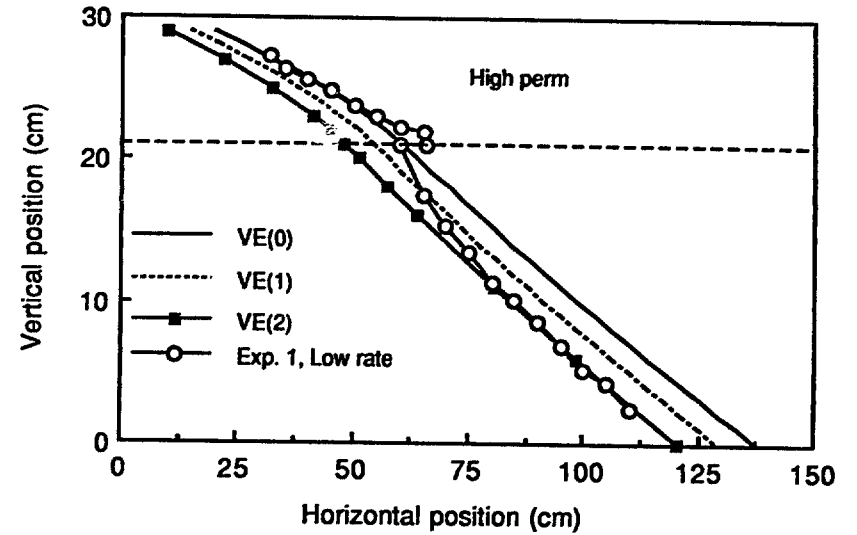


Figure 2 - Experiment 1

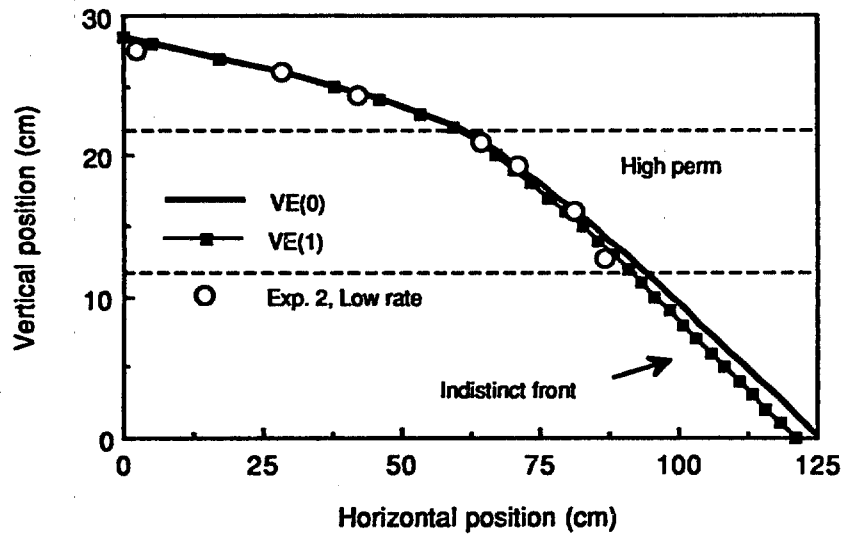


Figure 3 - Experiment 2

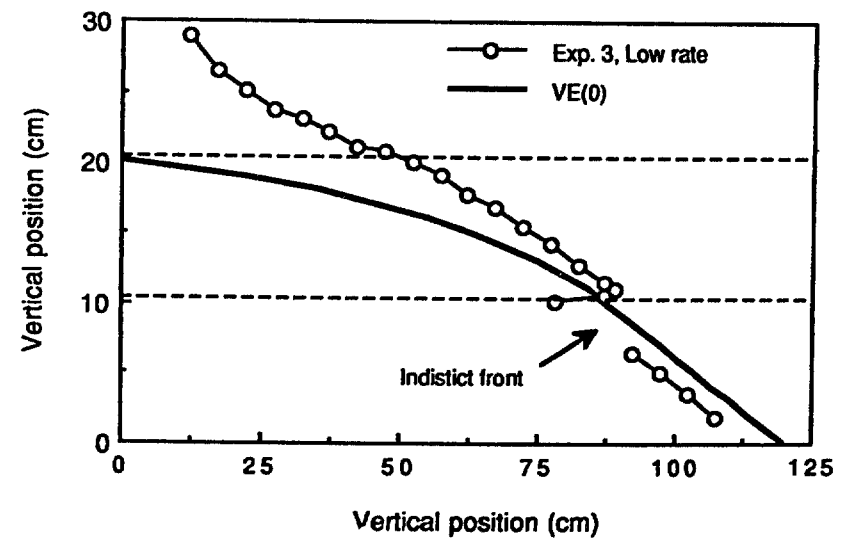


Figure 4 - Experiment 3

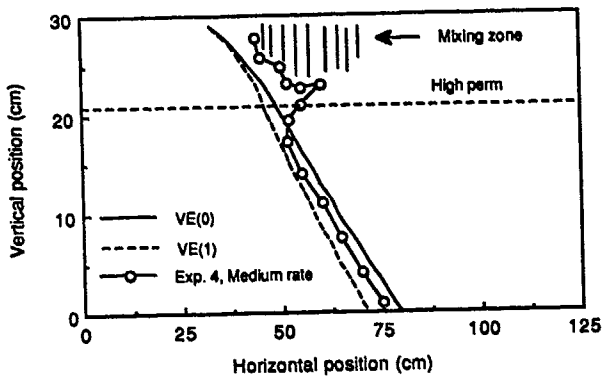


Figure 5 - Experiment 4

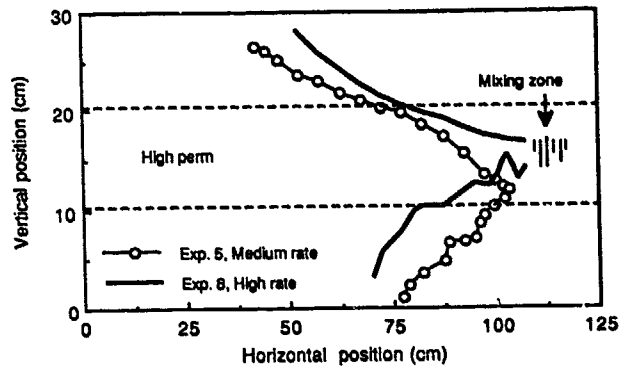


Figure 6 - Experiments 5 and 8

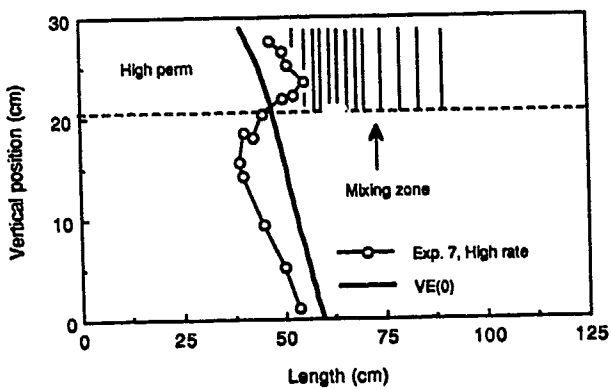


Figure 7 - Experiment 7

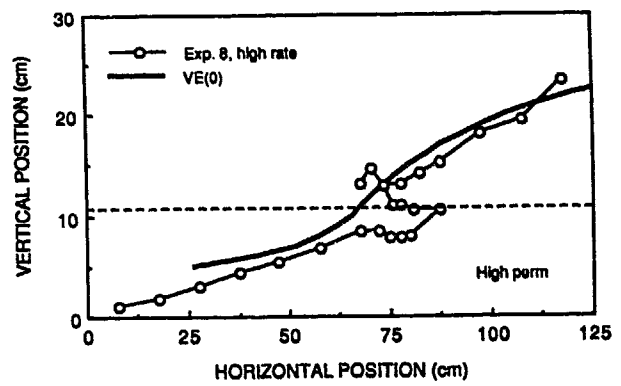


Figure 8 - Experiment 8, M > 1.

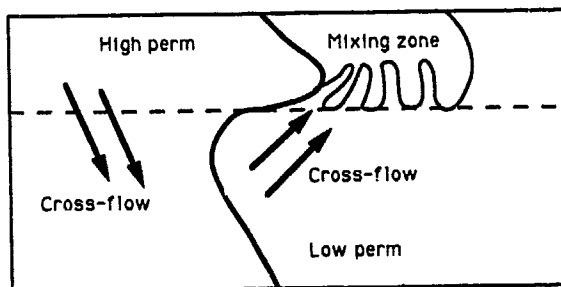


Figure 9 - Illustration of viscous mixing